

**Search for an effect of shell closure on nuclear dissipation via a neutron-multiplicity measurement**

Varinderjit Singh,<sup>1</sup> B. R. Behera,<sup>1,\*</sup> Maninder Kaur,<sup>1</sup> P. Sugathan,<sup>2</sup> K. S. Golda,<sup>2</sup> A. Jhingan,<sup>1,2</sup> Jhilam Sadhukhan,<sup>3</sup> Davinder Siwal,<sup>4</sup> S. Goyal,<sup>4</sup> S. Santra,<sup>5</sup> A. Kumar,<sup>1</sup> R. K. Bhowmik,<sup>2</sup> M. B. Chatterjee,<sup>2</sup> A. Saxena,<sup>5</sup> Santanu Pal,<sup>3</sup> and S. Kailas<sup>5</sup>

<sup>1</sup>*Department of Physics, Panjab University, Chandigarh 160014, India*

<sup>2</sup>*Inter University Accelerator Centre, New Delhi 110067, India*

<sup>3</sup>*Variable Energy Cyclotron Centre, 1/AF, Bidhan Nagar, Kolkata 700064, India*

<sup>4</sup>*Department of Physics and Astrophysics, Delhi University, Delhi 110007, India*

<sup>5</sup>*Nuclear Physics Division, Bhabha Atomic Research Centre, Mumbai 400085, India*

(Received 21 March 2012; published 13 July 2012)

The precision neutron multiplicity excitation function is measured for the first time for three isotopes across a major closed shell in order to investigate the shell effects on fission hindrance. Three isotopes of Fr ( $^{213,215,217}\text{Fr}$ ) are populated by fusion of  $^{19}\text{F}+^{194,196,198}\text{Pt}$  in the excitation energy range of 46.6–91.8 MeV. While  $^{213}\text{Fr}$  has a major neutron shell closure at  $N = 126$ ,  $^{215}\text{Fr}$  and  $^{217}\text{Fr}$  are away from the closed shell. It is found from the statistical model analysis of the experimental data that the strengths of nuclear dissipation for nuclei away from shell closure are very similar. On the other hand, the dissipation is relatively weaker for a shell-closed nucleus in comparison to adjacent nuclei away from shell closure.

DOI: [10.1103/PhysRevC.86.014609](https://doi.org/10.1103/PhysRevC.86.014609)

PACS number(s): 25.70.Jj, 25.70.Gh, 24.10.Pa

The phenomenon of dissipation is well known in the dynamics of macroscopic systems. Evidence for dissipation in strongly interacting small systems such as a nucleus has been accumulated from studies of nuclear dynamics at temperatures of the order of a few MeV in the past [1–4]. More recently, dissipative dynamics is also found to play a crucial role in the evolution of matter at extremely high densities and temperatures created in collisions between two heavy nuclei at ultrarelativistic energies [5]. Interestingly, Auerbach and Shlomo [6] subsequently pointed out that the strengths of the dissipation-to-entropy density ratios obtained from nuclear systems at low as well as at very high temperatures are very similar. Understanding dissipation is one of the challenges in present-day nuclear physics.

Dissipation in nuclear dynamics in the mean-field regime accounts for the coupling of the collective motion with the intrinsic nucleon degrees of freedom. The energy spectrum of intrinsic motion has a well-defined shell structure which is known to persist in an excited nucleus [7–10]. It is therefore of considerable interest to investigate the effect of shell structure on the strength of nuclear dissipation. In particular, a scan of nuclear dissipation across the neighborhood of a closed-shell nucleus can reveal the effect of shell closure. Specifically, we consider the dissipation which hinders the shape evolution of a compound nucleus from the ground state to the scission configuration.

The effect of shell closure on nuclear dissipation was examined earlier by Back *et al.* [11] by considering the evaporation residue cross sections of a number of nuclei having  $\geq 126$  neutrons. The compound nuclei which were considered, however, had different proton numbers, except for two thorium isotopes, and were formed using different projectiles on different targets in different experiments. It is,

however, desirable to choose compound nuclei for which either the neutron number or the proton number varies across a closed shell. It is, further, desirable to produce these compound nuclei using either the same projectile or the same target nucleus. For such cases, experimental observables can be interpreted rather unambiguously in terms of shell closure effects.

Guided by the above considerations, we performed an experiment to explore the effect of shell closure on nuclear dissipation through precision neutron multiplicity ( $M_{\text{pre}}$ ) measurement and the results are presented in this article. Three different isotopes of Fr were populated through fusion of the  $^{19}\text{F}$  projectile with the  $^{194,196,198}\text{Pt}$  target nuclei. Of the above compound nuclei,  $^{213}\text{Fr}$  contains neutron shell closure ( $N = 126$ ) and the other two are away from shell closure. The compound nuclei were formed in the excitation energy range of 46.6–91.8 MeV. Though  $M_{\text{pre}}$  has been measured for a number of systems previously [12] including  $^{28}\text{Si}+^{164,170}\text{Er}$  systems [13] over a limited number of beam energies, the present experiment is the first to measure  $M_{\text{pre}}$  from three compound nuclei which span a major shell closure and are formed with the same projectile nucleus.

The experiment was performed using the 15UD Pelletron + LINAC and the National Array of Neutron Detectors (NAND) facility at the Inter University Accelerator Centre (IUAC), New Delhi. A pulsed beam of  $^{19}\text{F}$  (repetition rate, 250 ns; FWHM,  $\sim 600$  ps) in the laboratory energy range of 92–141 MeV was bombarded on targets of  $^{194,196,198}\text{Pt}$ , resulting in the formation of the compound nuclei  $^{213,215,217}\text{Fr}$ . Pt targets (rolled foils of enrichment  $>98\%$  and thickness  $\sim 1.8$  mg/cm<sup>2</sup>) were kept at the center of a thin-walled (3 mm thickness) spherical scattering chamber of 60 cm diameter and were placed at 90° with respect to the beam. The fission fragments were measured in coincidence using a pair of position-sensitive multiwire proportional counter of active area  $5 \times 3$  in., kept at the folding angle on both sides of the beam axis, at a distance of 18.5 and 17.0 cm from the target

\*bivash@pu.ac.in

position, respectively. Neutrons were detected in coincidence with the fission events using 16 BC501 organic scintillator neutron detectors kept 2 m away from the target position. A hardware threshold of 0.5 MeV of neutron energy was applied to the neutron detector by calibrating it with the standard radioactive sources of  $^{137}\text{Cs}$  and  $^{60}\text{Co}$  [14]. Neutron and  $\gamma$  discrimination was performed by using both the time-of-flight technique and the pulse shape discrimination module based on the zero-crossover technique [15]. In order to keep the background at the minimum level, the beam dump was kept at a distance of 4.2 m from the target position and was shielded with paraffin blocks and lead bricks. To estimate the level of background in the neutron spectra, data were also taken with a blank target holder. It was observed that the background in the neutron spectra was negligible. The efficiency of the neutron detectors was obtained experimentally by measuring the neutron spectra of a calibrated  $^{252}\text{Cf}$  source kept at the target position.

Neutrons detected in coincidence with the fission fragments originate from three moving sources, namely, evaporation from the compound nucleus (pre-scission neutrons) and evaporation from the two fission fragments (post-scission neutrons). The theoretical expression for the total neutron energy spectrum can be given as the sum of all three sources in the form

$$\begin{aligned} & \frac{d^2 M_n}{dE_n d\Omega_n} \\ &= \sum_{i=1}^3 \frac{M_n^i \sqrt{E_n}}{2(\pi T_i)^{3/2}} \exp \left[ -\frac{E_n - 2\sqrt{\varepsilon_i E_n} \cos \Phi_i + \varepsilon_i}{T_i} \right], \end{aligned} \quad (1)$$

where  $\varepsilon_i$ ,  $T_i$ , and  $M_n^i$  are, respectively, the energy per nucleon, the temperature, and the multiplicity of the neutron source  $i$ .  $E_n$  is the energy of the neutrons and  $\phi_i$  is the relative angle between the neutron detector and the source  $i$ . This expression is known as the Watt expression [16]. The post-scission neutron multiplicity ( $M_{\text{post}}$ ) was obtained by assuming the same neutron multiplicity and temperature ( $T$ ) for both fission fragments. Thus the total neutron multiplicity can be given as  $M_{\text{tot}} = M_{\text{pre}} + 2M_{\text{post}}$ . For estimating the neutron multiplicity contribution from each source, the efficiency-corrected neutron energy spectra of all the detectors were fitted simultaneously using the Watt expression following the  $\chi^2$  minimization procedure, treating  $M_{\text{pre}}$ ,  $M_{\text{post}}$ ,  $T_{\text{pre}}$ , and  $T_{\text{post}}$  as free parameters. The same process was also repeated by fixing the  $T_{\text{pre}} = \frac{11}{12} \sqrt{\frac{E^*}{a}}$  [17,18] (where  $E^*$  is the initial excitation energy and  $a$  is the nuclear level density parameter, taken to be  $A_{\text{CN}}/9$ ). The results obtained in both cases were found to be in agreement. The pre-scission ( $M_{\text{pre}}$ ) and total ( $M_{\text{tot}}$ ) neutron multiplicities thus obtained for different compound nuclei are given in Fig. 1. The pre-scission neutron multiplicities for different isotopes of Fr are also shown in the same plot in Fig. 2(a) for comparison. It can be noted immediately from that figure that the measured multiplicity variation from  $^{213}\text{Fr}$  to  $^{215}\text{Fr}$  is greater than that between  $^{215}\text{Fr}$  and  $^{217}\text{Fr}$ . Other factors such as excitation energies and atomic numbers being the same in all three compound nuclei, the above observation

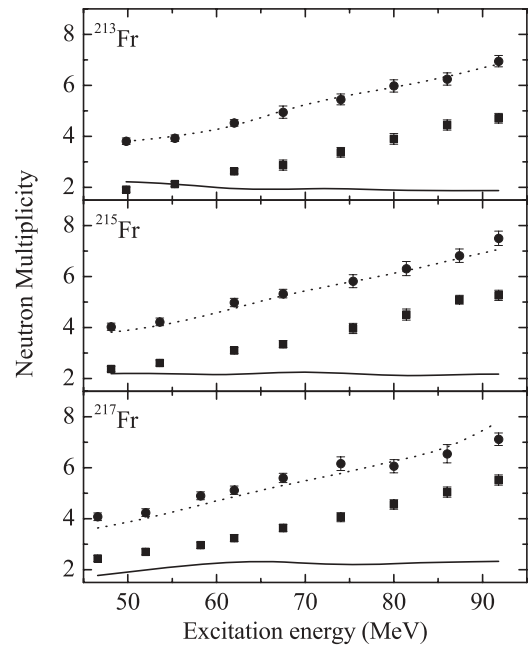


FIG. 1. Experimental pre-scission (filled square) and total (filled circle) neutron multiplicities for different systems. Statistical model results for pre-scission (solid line) and total (dashed line) neutron multiplicities with  $\beta = 0$  are also shown.

suggests an effect of shell closure in  $^{213}\text{Fr}$  on the multiplicity of pre-scission neutrons.

In order to investigate the shell effects on the pre-scission neutron excitation function, we next analyzed the experimental data using the statistical model for decay of a compound nucleus. We considered evaporation of neutrons, protons,  $\alpha$  particles and the statistical giant dipole  $\gamma$  rays as the decay channels of an excited compound nucleus, in addition to fission. The fate of a compound nucleus is determined by the competition between its different decay modes. The intensity of different decay modes depends critically on the density of levels of the parent and the daughter nuclei. The level density in turn is a sensitive function of the level density parameter ( $a$ ), which was taken from the work of Ignatyuk *et al.* [19], who proposed a form which includes shell effects at low excitation energies and goes over to its asymptotic form at high excitation energies; it is given as

$$a(E^*) = \bar{a} \left( 1 + \frac{f(E^*)}{E^*} \delta W \right) \quad (2)$$

with

$$f(E^*) = 1 - \exp(-E^*/E_d), \quad (3)$$

where  $\bar{a}$  is the asymptotic level density and  $E_d$  is a parameter which decides the rate at which the shell effects disappear with an increase in the excitation energy ( $E^*$ ). A value of 18.5 MeV was used for  $E_d$ , which was obtained from an analysis of  $s$ -wave neutron resonances [20]. The shell correction term  $\delta W$  is given as the difference between the experimental and the liquid-drop model (LDM) masses ( $\delta W = M_{\text{exp}} - M_{\text{LDM}}$ ). The asymptotic level density  $\bar{a}$  was taken from Ref. [20]. For the fission width, we used the following expression obtained by

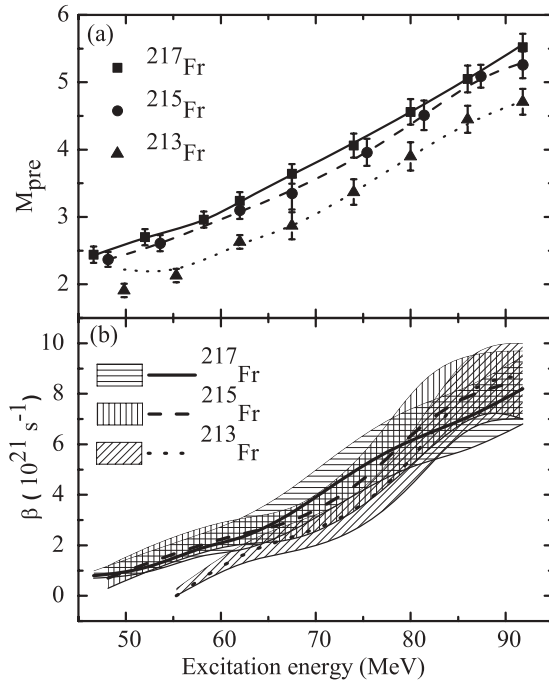


FIG. 2. (a) Experimental pre-scission neutron multiplicity (symbols) for different systems with statistical model fits (lines) when shell effects are included in the calculation. (b) Best-fit values (lines) of  $\beta$ . Hatched areas represent the uncertainty in  $\beta$  associated with the experimental error in  $M_{\text{pre}}$ .

Kramers [21], considering a dissipative dynamics for fission,

$$\Gamma_K = \frac{\hbar\omega_g}{2\pi} e^{-V_B/T} \left\{ \sqrt{1 + \left(\frac{\beta}{2\omega_s}\right)^2} - \frac{\beta}{2\omega_s} \right\}, \quad (4)$$

where  $\beta$  is the reduced dissipation coefficient (ratio of dissipation coefficient to inertia) and  $\omega_g$  and  $\omega_s$  are the local frequencies of the harmonic oscillator potentials which osculate the nuclear potential in the ground state and the saddle configuration, respectively [22]. The fission barrier height and the temperature of the compound nucleus are, respectively, denoted by  $V_B$  and  $T$ . Taking shell effects into account, the fission barrier was further modified as [19]

$$V_B(T) = V_{\text{LDM}} - \delta W \exp(-E^*/E_d), \quad (5)$$

where  $V_{\text{LDM}}$  is the fission barrier from the finite-range rotating LDM potential [23]. It may be noted here that the shell correction was applied only to the ground-state mass, and it was assumed that the shell correction at the saddle deformation can be neglected [24–26]. The above assumption of neglecting the shell correction at the saddle deformation follows from the topographical argument of Myers and Swiatecki [24], which states that the undulations in the potential landscape at the saddle owing to shell effects do not make any difference in the dynamical fission path across the saddle with respect to the macroscopic potential. It is of further interest to note that the fission barrier heights from microscopic calculations also show a temperature dependence similar to that given in Eq. (4) [27].

In the statistical model calculation, the decay of a compound nucleus is simulated using the Monte Carlo technique, where the various decay widths are considered at successive time intervals. The effect of the transient time or the buildup time period that elapses before the stationary value of Kramers' fission width is reached was taken into account by using the time-dependent fission width given by Bhatt *et al.* [28]. Further, the number of emitted particles during the saddle-to-scission transition was also calculated using the saddle-to-scission time period given in Ref. [29].

Taking into account the shell effects in the level densities and the fission barriers, the pre-scission and the total neutron multiplicities were calculated, and a comparison with the experimental values is shown in Fig. 1 for  $\beta = 0$ . It is demonstrated that the pre-scission neutron multiplicities are underestimated for all cases except the one at the lowest excitation energy of  $^{213}\text{Fr}$ . It may be pointed out that the statistical model predictions with  $\beta = 0$  for  $M_{\text{pre}}$  should not be larger than the experimental values, and although the input level density parameters can be adjusted to bring down the calculated  $M_{\text{pre}}$  value for  $^{213}\text{Fr}$  at 50 MeV excitation, we preferred to use the standard parameter set for level density in our calculation, as the deviation concerns only one data point by a marginal amount. It may further be noted that although the  $M_{\text{pre}}$  values are underpredicted, the multiplicities of the total number of neutrons are reasonably well reproduced. This is a consequence of the balance of the excitation energies carried away by the pre-scission and the post-scission neutrons, as, together, they account for most of the initial excitation energy of the compound nucleus.

We next fitted the experimental  $M_{\text{pre}}$  value at each excitation energy with the statistical model result using  $\beta$  as a free parameter. Figure 2(a) shows the fitted values of  $M_{\text{pre}}$  along with the experimental numbers. The corresponding values of  $\beta$  are given in Fig. 2(b). In that plot, the hatched area for each nucleus corresponds to the uncertainty in the fitted  $\beta$  values owing to error in the experimental  $M_{\text{pre}}$ . It is shown that the  $\beta$  values for  $^{215}\text{Fr}$  and  $^{217}\text{Fr}$  are remarkably close within the limits of uncertainty over the entire excitation energy range. The shell structures of the above two isotopes of Fr are also very similar, each having a partially occupied  $1g_{9/2}$  neutron shell after the shell gap at neutron number 126. On the other hand, the dissipation strength required for  $^{213}\text{Fr}$  is clearly lower than those for  $^{215}\text{Fr}$  and  $^{217}\text{Fr}$  at lower excitation energies, although all three become close at higher excitation energies. With a major shell closure with 126 neutrons, the shell structure of  $^{213}\text{Fr}$  is very distinct from those of  $^{215,217}\text{Fr}$ . Recalling that the shell structure can influence the level density, fission barrier, and strength of dissipation, the above observation regarding less dissipation for  $^{213}\text{Fr}$  can be attributed solely to its shell structure, as shell effects in the level density and the fission barrier are already included in the calculation. We thus arrive at the following picture regarding shell effects on dissipation. While the reduced dissipation strength varies marginally among nuclei which are away from shell closure, it is suppressed for closed-shell nuclei at low excitations. The above feature can also be expected from the microscopic theories of one-body dissipation [30,31], where incoherent particle-hole excitation by a time-dependent

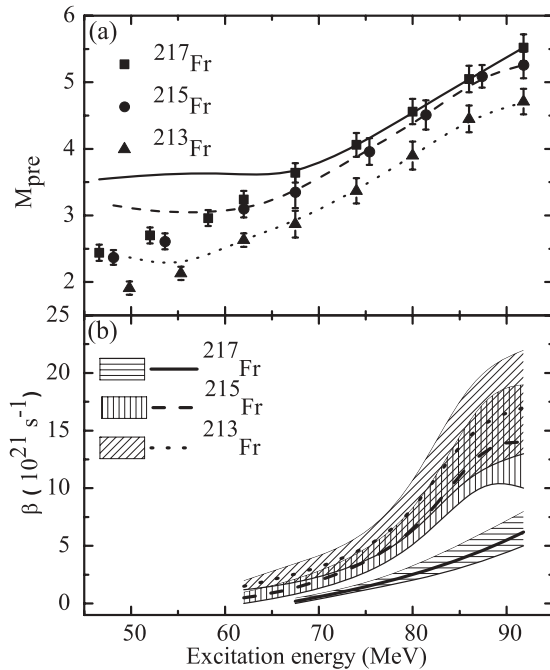


FIG. 3. Same as Fig. 2 except the statistical model calculations were performed excluding shell effects.

mean field causes dissipation. Particle-hole excitation being easier for non-closed-shell nuclei than for closed-shell nuclei, the former is expected to be more dissipative than the latter. The present results provide phenomenological evidence of the above expectation.

Figure 2(b) also shows a strong (initial) excitation energy dependence of  $\beta$ . Though the excitation energy dependence of nuclear dissipation is not yet clearly understood, it is usually attributed to several factors, which include the neglect of higher order terms in microscopic derivations of dissipation [32], shape dependence of dissipation [33], inadequacies in fission modeling [34], and need for a better treatment of the inertia [10]. We feel, however, that the inclusion of the above effects in nuclear dissipation will not alter the relative strengths of dissipation at each excitation energy and the shell closure effects will persist. Evidently, more work in this direction is required in future.

We next performed statistical model calculations without considering shell effects, and Fig. 3 shows the best-fit  $M_{\text{pre}}$  and the corresponding  $\beta$  values. It is curious to observe that  $M_{\text{pre}}$  cannot be fitted at all at low excitation energies for all three Fr isotopes. It is further demonstrated that the best-fit  $\beta$  values for different isotopes are quite different, in contrast to those obtained with shell effects as given in Fig. 2. In order to seek an explanation for the above behavior, we first examine the nature of the neutron width with and without the shell correction. We note that the neutron widths for the different isotopes respond differently when the shell effects are turned off in the level density parameter. Because the neutron width is essentially determined by the ratio of the level densities of the daughter and the parent nuclei, inclusion of the shell correction increases or decreases the neutron width, depending upon the relative magnitudes of the shell correction in the daughter and

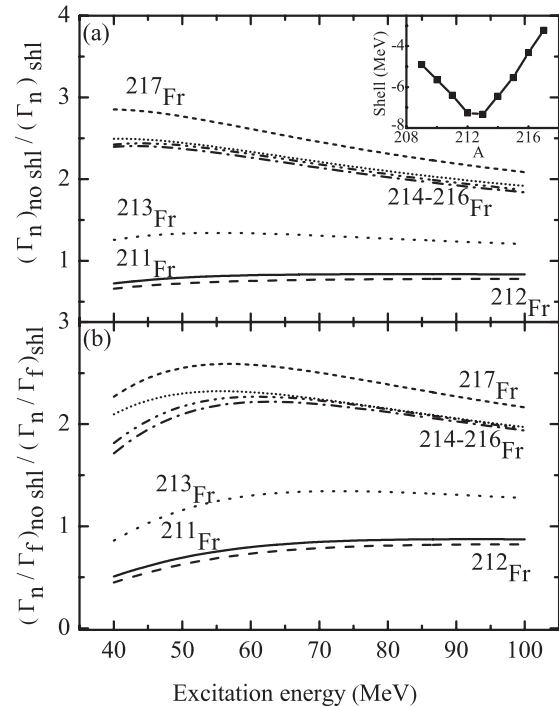


FIG. 4. (a) Comparison of neutron widths without and with shell effects for different isotopes of Fr. (b) A similar comparison for the neutron-to-fission width ratio. Widths are calculated for compound nuclei with spin  $40\hbar$ . Inset: Variation of shell correction with mass number for Fr isotopes.

the parent nuclei. As a consequence of the systematic variation of the shell correction for the Fr isotopes across the shell closure at  $N = 126$  (inset in Fig. 4),  $\Gamma_n$  and  $\Gamma_n / \Gamma_f$  become modified as illustrated in Fig. 4. An increase in the  $\Gamma_n / \Gamma_f$  ratio for  $^{214-217}\text{Fr}$  results in an enhancement of neutron multiplicity for  $^{217}\text{Fr}$  when shell effects are not included in the calculation. The enhancement is so pronounced at lower excitation energies that even the largest fission width with  $\beta = 0$  is unable to reproduce the experimental multiplicity in Fig. 3. The above enhancement also reduces the best-fit  $\beta$  values in comparison to those in Fig. 2 at higher excitation energies for  $^{217}\text{Fr}$ . On the other hand, a decrease in the  $\Gamma_n / \Gamma_f$  ratio for  $^{212}\text{Fr}$  and lighter isotopes causes a suppression of neutron multiplicity for  $^{213}\text{Fr}$ , which in turn demands a stronger fission hindrance in order to fit the experimental data. Therefore, the fitted  $\beta$  values are much larger than the values obtained with shell effects. For  $^{215}\text{Fr}$ , the  $\Gamma_n / \Gamma_f$  ratio increases for some and decreases for other Fr compound nuclei which are encountered during successive neutron emission. The  $\beta$  values for  $^{215}\text{Fr}$  therefore lie in between those for  $^{213}\text{Fr}$  and those for  $^{217}\text{Fr}$ . Thus, the large variation in  $\beta$  among the three nuclei can be attributed to the neglect of shell effects. This, in turn, establishes the importance of the inclusion of shell effects in statistical model calculations in order to obtain a consistent picture of nuclear dissipation.

In summary, precission neutron excitation functions have been measured for compound nuclei  $^{213,215,217}\text{Fr}$  and analyzed using the statistical model. We find that the strengths of the reduced dissipation coefficient for nuclei which are away from

shell closure are very similar, though it is suppressed for closed-shell nuclei at low excitations. This indicates that the shell-assisted increase in the survival probability of closed-shell compound nuclei can be offset to some extent owing to the reduction in dissipation coefficient. This may adversely affect the synthesis of superheavy elements.

The authors acknowledge the support of the Pelletron-Linac accelerator crew of IUAC, New Delhi, for the excellent beam quality throughout the experiment. The financial

support from the Council of Scientific and Industrial Research (CSIR), Government of India, in terms of a grant from the Shyama Prasad Mukherjee program to one of the authors (V.S.) is gratefully acknowledged. B.R.B. acknowledges the Department of Atomic Energy (DAE), Government of India, for a DAE young scientist research grant (YSRA). Calculations were performed at the High-Performance Computing Center (HPCC) of the Department of Physics, Panjab University, Chandigarh.

- 
- [1] K. T. R. Davies *et al.*, *Phys. Rev. C* **13**, 2385 (1976).  
 [2] K. Thomas, R. Davies, A. J. Sierk, and J. R. Nix, *Phys. Rev. C* **28**, 679 (1983).  
 [3] D. H. E. Gross and H. Kalinowski, *Phys. Rep.* **45**, 175 (1978).  
 [4] M. Thoennessen and G. F. Bertsch, *Phys. Rev. Lett.* **71**, 4303 (1993).  
 [5] T. Schafer and D. Teaney, *Rep. Prog. Phys.* **72**, 126001 (2009).  
 [6] N. Auerbach and S. Shlomo, *Phys. Rev. Lett.* **103**, 172501 (2009).  
 [7] J. L. Egidio, L. M. Robledo, and V. Martin, *Phys. Rev. Lett.* **85**, 26 (2000).  
 [8] J. C. Pei, W. Nazarewicz, J. A. Sheikh, and A. K. Kerman, *Phys. Rev. Lett.* **102**, 192501 (2009).  
 [9] A. V. Ignatyuk *et al.*, *Nucl. Phys. A* **346**, 191 (1980).  
 [10] F. A. Ivanyuk and H. Hofmann, *Nucl. Phys. A* **657**, 19 (1999).  
 [11] B. B. Back *et al.*, *Phys. Rev. C* **60**, 044602 (1999).  
 [12] D. J. Hinde *et al.*, *Nucl. Phys. A* **452**, 550 (1986).  
 [13] J. O. Newton *et al.*, *Nucl. Phys. A* **483**, 126 (1988).  
 [14] T. G. Masterson, *Nucl. Instrum. Methods* **88**, 61 (1970).  
 [15] S. Venkataramanan *et al.*, *Nucl. Instrum. Methods A* **596**, 248 (2008).  
 [16] D. Hilscher *et al.*, *Phys. Rev. C* **20**, 576 (1979).  
 [17] K. J. Le Couteur and D. W. Lang, *Nucl. Phys.* **13**, 32 (1959).  
 [18] D. W. Lang, *Nucl. Phys.* **53**, 113 (1964).  
 [19] A. V. Ignatyuk *et al.*, *Yad. Fiz.* **21**, 485 (1975) [*Sov. J. Nucl. Phys.* **21**, 255 (1975)].  
 [20] W. Reisdorf, *Z. Phys. A* **300**, 227 (1981).  
 [21] H. A. Kramers, *Physica (Amsterdam)* **7**, 284 (1940).  
 [22] J. Sadhukhan and S. Pal, *Phys. Rev. C* **79**, 064606 (2009).  
 [23] A. J. Sierk, *Phys. Rev. C* **33**, 2039 (1986).  
 [24] W. D. Myers and W. J. Swiatecki, *Nucl. Phys. A* **601**, 141 (1996).  
 [25] A. V. Ignatyuk, M. G. Itkis, and S. I. Mulgin, *Fiz. Elem. Chastits At. Yadra* **16**, 709 (1985) [*Sov. J. Part. Nuclei* **16**, 307 (1985)].  
 [26] V. Yu. Denisov and S. Hofmann, *Phys. Rev. C* **61**, 034606 (2000).  
 [27] J. A. Sheikh, W. Nazarewicz, and J. C. Pei, *Phys. Rev. C* **80**, 011302(R) (2009).  
 [28] K. H. Bhatt, P. Grange, and B. Hiller, *Phys. Rev. C* **33**, 954 (1986).  
 [29] H. Hofmann and J. R. Nix, *Phys. Lett. B* **122**, 117 (1983).  
 [30] H. Hofmann and P. J. Siemens, *Nucl. Phys. A* **257**, 165 (1976).  
 [31] S. Pal and N. K. Ganguly, *Nucl. Phys. A* **370**, 175 (1981).  
 [32] J. Blocki *et al.*, *Ann. Phys.* **113**, 330 (1978).  
 [33] I. Dioszegi, N. P. Shaw, I. Mazumdar, A. Hatzikoutelis, and P. Paul, *Phys. Rev. C* **61**, 024613 (2000).  
 [34] J. P. Lestone and S. G. McCalla, *Phys. Rev. C* **79**, 044611 (2009).